

## The high-pressure synthesis of lawsonite in the MORB+H<sub>2</sub>O system

KAZUAKI OKAMOTO\* AND SHIGENORI MARUYAMA

Department of Earth and Planetary Sciences, Tokyo Institute of Technology, O-okayama 2-12-1, Meguro-Ku, Tokyo 152-8551, Japan

### ABSTRACT

Lawsonite is an important water reservoir in subducting oceanic crust below the amphibole dehydration depth ~70 km. To determine the maximum pressure stability of lawsonite in the MORB+H<sub>2</sub>O system, experiments were carried out using a 1000 ton uniaxial multi-anvil apparatus (SPI-1000). Mixtures of synthetic gel+2wt% H<sub>2</sub>O were used for the starting materials with the average MORB composition. Experimental *P-T* conditions were *T* = 700–900 °C and *P* = 5.5–13.5 GPa. Run durations were 12 and 24 h.

Lawsonite was synthesized stably up to 10 GPa and *T* < 700 °C in the stishovite stability field, and <900 °C at 8 GPa and 750 °C at 5.5 GPa in the coesite stability field, with a steep positive slope for the lawsonite-out reaction. The lawsonite-out reaction in the coesite stability field changes to have a gentle negative slope in the stishovite stability field. The reaction leading to the disappearance of lawsonite is a continuous reaction due to the compositional enlargement of garnet toward the grossular end-member with increasing *T* and *P*. Lawsonite disappears when the tie line connecting grossular-rich garnet with omphacitic clinopyroxene reaches the bulk composition on the conventional AC(FM) ternary diagram.

### INTRODUCTION

The role of water in the genesis of magma in subduction zone environments has been widely recognized (e.g., Wyllie 1988). Magma in subduction zones has been attributed either to direct melting of the hydrous slab (e.g., Nicholls and Ringwood 1973; Wyllie and Sekine 1982; Brophy and Marsh 1986) or to the release of fluids from the slab to decrease the melting temperature of the mantle wedge (e.g., Ringwood 1975; Delany and Helgeson 1978; Tatsumi et al. 1986). The dehydration due to isobaric amphibole breakdown, traditionally taken as the amphibolite-eclogite transformation reaction, is believed to provide the water necessary to trigger partial melting of the overlying mantle wedge. However, several high-pressure hydrous minerals have been documented to be stable at coesite and diamond isograds in many ultrahigh-pressure metamorphic terranes (see reviews by, e.g., Liou et al. 1994; Chopin and Sobolev 1995; Schreyer 1995). Recent experimental studies (Schreyer 1988; Poli 1993; Poli and Schmidt 1995) have shown that hydrous phases such as lawsonite, chloritoid, staurolite, phengite, and zoisite-clinozoisite are valid candidates in subducting oceanic crust as minerals that may transport water to depths greater than the amphibole stability field.

Lawsonite is an important ultrahigh-pressure (UHP) hydrous mineral that forms along a cold geothermal gradient. It is present commonly in metabasites and metagreywackes, and is less common in metapelites formed under blueschist facies conditions. However, lawsonite is

rare in rocks formed under eclogite facies conditions, there being just four well-known examples. One is from lawsonite-bearing eclogite nodules from Garnet Ridge, Arizona (Helmstaedt and Doig 1975; Helmstaedt and Schulze 1988), and the other three are from Corsica (Caron and Pequignot 1986), Pinchi Lake, British Columbia (Ghent et al. 1993), and Java Island (Parkinson et al. 1998). All of these lawsonite-bearing eclogites occur sporadically, and are never exposed as a coherent regional metamorphic belt. Experimental evidence, on the other hand, shows that lawsonite should occur under conditions where the regional geothermal gradient is low.

The stability field of lawsonite has been determined using a multi-anvil apparatus in the CASH system (Schmidt and Poli 1994; Pawley 1994). Conflicting results show that lawsonite of its own bulk composition is stable to a pressure of either 13.5 GPa at 800 °C (Pawley 1994) or 12 GPa at 800 °C (Schmidt 1995), and between 6.5 and 12 GPa at 1000 °C (Pawley 1994). In the NCFMASH and KNCFMASH systems, lawsonite is stable at 6 GPa and 800 °C (in a basalt system) and 870 °C (andesite system) (Poli and Schmidt 1995). However, the maximum *P, T* stability of lawsonite in the MORB+H<sub>2</sub>O system has not been determined (Fig. 1).

If the subduction zone geotherms are cold enough, lawsonite may be an important water reservoir in slabs subducting to depths greater than that of amphibole dehydration (above 6 GPa). It is therefore important to determine the precise dehydration conditions of lawsonite in the subducting oceanic plate to clarify the mechanism by which water may be transported into the deep mantle.

\* E-mail: kokamoto@geo.titech.ac.jp

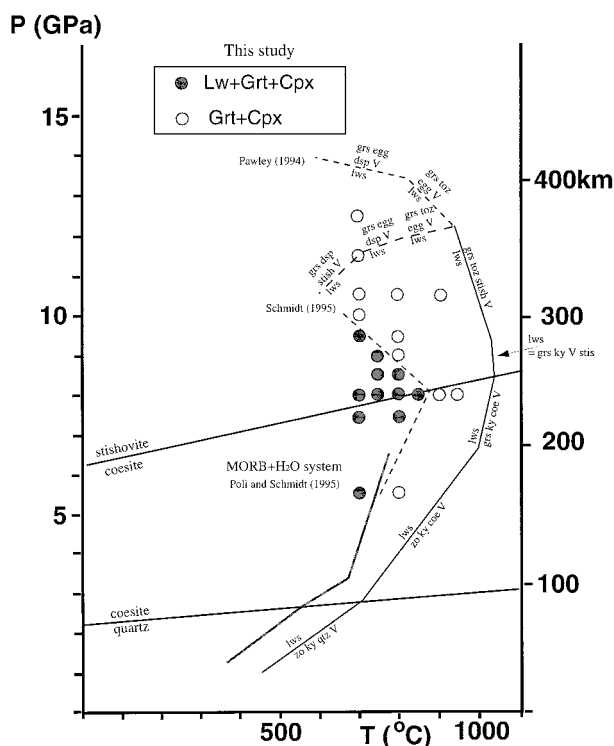


**FIGURE 1.** Stability fields of lawsonite in CASH and MORB+H<sub>2</sub>O system. Thin lines delineate the stability fields of lawsonite in the CASH system (Pawley 1994; Schmidt 1995) and the quartz, coesite, and stishovite stability field (Bohlen and Boettcher 1982; Zhang et al. 1996). The thick lines delineate the stability field of lawsonite in the MORB+H<sub>2</sub>O system below 6 GPa (Poli and Schmidt 1995) and the thin dashed lines delineate the stability field of lawsonite above 6 GPa from this study. Abbreviations: lws = lawsonite, zo = zoisite, qtz = quartz, V = vapor, ky = kyanite, coe = coesite, grs = grossular, toz = topaz-OH, stish = stishovite, egg = phase egg, and dsp = diasporite.

Several recent experiments suggest that H<sub>2</sub>O may be stored at higher pressures in several other hydrous phases (phase-A, phase-E, hydrous- $\beta$ , and hydrous- $\gamma$ ) in the upper mantle transition zone (e.g., Kawamoto et al. 1996; Smyth and Kawamoto 1997; Inoue et al. 1995). Lawsonite may therefore be key in transporting water to depths where dense hydrous magnesium silicates (DHMS hereafter) are stabilized. The aim of this study was to determine the maximum pressure stability of lawsonite in the MORB+H<sub>2</sub>O system.

#### EXPERIMENTAL PROCEDURE

Experiments were carried out using a 1000 ton uniaxial multi-anvil apparatus (SPI-1000) at the Tokyo Institute of Technology. The SPI-1000 was designed by E. Takahashi and constructed by the Riken Co. in 1991 and installed in his lab at the Tokyo Institute of Technology. The multi-anvils are doubled-stage, and bucket-type guide blocks (neither split sphere nor cylinder) were newly designed to drive the cubic-octahedral anvils (see detail in Taka-

hashi et al. 1993). Similar to double-stage multi-anvil presses in other laboratories (Ito et al. 1984), pressure media of various octahedral sizes were used in the SPI-1000 by changing the final truncation size of the tungsten carbide anvils. The assembled tungsten carbide anvils leave an octahedral cavity. Pressure calibrations of this apparatus were shown in Takahashi et al. (1993). In the present experiments, octahedral MgO pressure media of 18 mm edge length (18M) and 14 mm edge length (14M) were used in which a few percent of Cr<sub>2</sub>O<sub>3</sub> was added to reduce thermal conductivity. Furnace assemblages are shown in Figure 1 of Okamoto and Maruyama (1988). A LaCrO<sub>3</sub> furnace was used with the ZrO<sub>2</sub> sleeve for heat insulation in the 18M assembly, although no ZrO<sub>2</sub> sleeve was used in the 14M octahedron. A gold capsule containing 0.3 mg of starting material was used. Temperature was measured with W<sub>95</sub>-Re<sub>5</sub>/W<sub>74</sub>-Re<sub>26</sub> thermocouples. Recorded pressure is considered to be accurate to  $\pm 0.2$  GPa.

Experiments were heated from room temperature to 900 °C or higher within approximately 30 min and quenched to 100 °C in approximately 30 s. In most experiments, the total compression time was approximately 2 h. Fluctuations in the oil pressure and the furnace temperature were on the order of 0.1 MPa and 3 °C, respectively (cf. Takahashi et al. 1993). The sealed gold capsules retained H<sub>2</sub>O in all runs.

At the end of each experiment, the capsule was sectioned longitudinally using a Buehler Isomet saw and mounted in epoxy. The cut surface was vacuum impregnated with epoxy to cement porous crystal aggregates.

Mineral identification, phase relations, and chemical analyses of major elements for run products were performed with a microfocused X-ray diffraction (XRD), laser Raman spectrometer (NRS-2000), SEM-EDS, and electron probe microanalyzer (JEOL-JXA8800). In each capsule, only the top portion of the sample within 100  $\mu$ m nearest to the thermocouple was analyzed to minimize the temperature error. Textural relations and chemical heterogeneity of garnet and clinopyroxene were examined using backscattered electron (BSE) imaging and SEM-EDS. All microprobe analyses were performed with an accelerating voltage of 15 kV, 12 nA beam current, and counting times of 10–20 s. A full oxide ZAF correction was applied to all analysis.

Laser Raman spectroscopy was used to identify the SiO<sub>2</sub> polymorph and fine-grained phases in run products. The ambient laser Raman spectra were recorded from 200 to 2000 cm<sup>-1</sup> for all run products. All spectra were obtained with the 514.5 nm line from a Spectra Physics model 2020 argon ion laser using 10 mW power at the samples, and 2 accumulations at 3 s integration time. A 50 $\times$  microscope objective was used to focus the laser beam and to collect the scattered light. The focused laser spot on the samples was estimated to be approximately 1 mm in diameter.

Micro-focused X-ray diffraction analysis was carried out to identify minerals in run products. The focused X-ray on the samples was approximately 50  $\mu$ m in diameter

**TABLE 1.** Major element composition (wt%) of the starting material determined by XRF analysis

SiO <sub>2</sub>	50.63
TiO <sub>2</sub>	1.74
Al <sub>2</sub> O <sub>3</sub>	14.72
Fe <sub>2</sub> O <sub>3</sub>	11.09
MgO	7.61
CaO	11.13
Na <sub>2</sub> O	2.91
K <sub>2</sub> O	0.13

Notes: Analysis normalized to 100% (anhydrous) with total iron as Fe<sub>2</sub>O<sub>3</sub>.

on the polished surface of the run charges. XRD patterns were obtained using Cr radiation (40kV, 30mA). The X-ray signals were taken between 20° and 140° 2θ at intervals of 0.02° and 1 s interval.

### STARTING MATERIALS

A gel+2wt% H<sub>2</sub>O was used in all experiments. The bulk composition of the gel represents the average composition of MORB after Shido and Miyashiro (1971) (Table 1). A hydrous glass+seed crystals and a synthetic amphibolite were both made from the gel+2wt% H<sub>2</sub>O. A hydrous glass was made using a gas apparatus and a synthetic amphibolite was made using a piston cylinder.

### EXPERIMENTAL RESULTS

Twenty-five runs were conducted. Experimental temperatures were from 700 °C up to 950 °C. Experimental pressures were from 5.5 to 13.5 GPa. Run durations were 12 and 24 h. The experimental results are listed in Table

2 and plotted on a *P-T* diagram in Figure 1. Run products were composed mainly of garnet, clinopyroxene, SiO<sub>2</sub> phase (coesite or stishovite), and ± lawsonite. Lawsonite was not observed at temperatures higher than 750 °C at 5.5 GPa, and at 8 GPa the boundary line passes between 850 °C and 900 °C. This indicates that the lawsonite-out reaction line has a positive steep *P-T* slope (0.75 GPa/100 °C). Above 8 GPa, however, the lawsonite-out reaction has a negative *P-T* slope (−0.13 GPa/100 °C) as it passes between 9.5 and 10.0 GPa at 700 °C, and between 8.5 and 9.0 GPa at 800 °C. Minor phengite, corundum, and glass were observed in several charges. The glass possibly originated from a supercritical fluid that dissolved considerable amounts of rock-forming components as described later in detail.

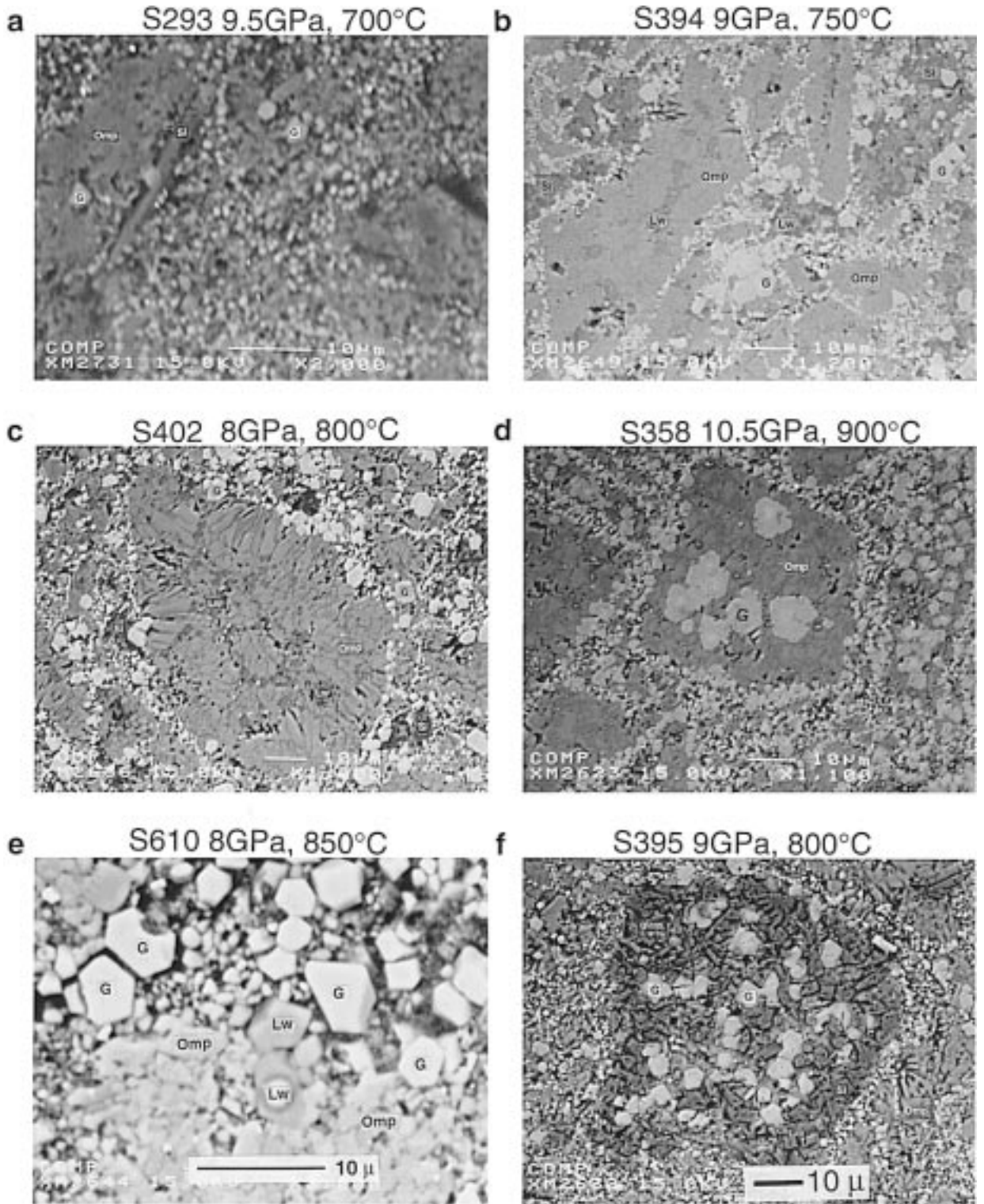
In BSE images, several different textures suggesting equilibrium or proving disequilibrium were observed. Textures in all run charges are characterized by clinopyroxene porphyroblasts in a fine-grained matrix composed of garnet, clinopyroxene, SiO<sub>2</sub> polymorph, and ± lawsonite. No garnet porphyroblasts were observed.

With increasing pressure and temperature, clinopyroxene increases in size from ~10 to 80 μm, whereas garnet and lawsonite remain generally <10 μm (Fig. 2a). Lawsonite is typically very fine grained and appears in the matrix, forming composite grains with porphyroblastic clinopyroxene (Fig. 2b). Some rounded reaction margins are observed for clinopyroxene at high temperature (Fig. 2c). The clinopyroxenes are fragmented, recognized as aggregates of fiber shaped or sheaved crystals. Idiomorphic garnet crystals are commonly included in clinopy-

**TABLE 2.** *P-T* condition, run duration, and mineral assemblages of run products

Run code	Pressure (GPa)	Temperature (°C)	Starting material	Grt	Omp	SiO <sub>2</sub>	Lws	Phen	Crn	Glass
S290	5.5	700	A	○	○	○	○	○	—	—
S280	7.5	700	C	○	○	○	○	—	—	—
S611	8	700	B	○	○	○	○	—	—	—
S293	9.5	700	A	○	○	○	○	—	—	—
S362	9.5	700	B	○	○	○	○	—	—	—
S393	10	700	B	○	○	○	—	—	—	○
S706	10	700	S-611 + S-362	○	○	○	—	—	—	—
S349	10.5	700	B	○	○	○	—	—	—	—
S345	11.5	700	B	○	○	○	—	—	—	—
S347	12.5	700	B	○	○	○	—	—	—	○
S348	13.5	700	B	○	○	○	—	—	—	—
S400	8	750	B	○	○	○	○	—	—	—
S398	8.5	750	B	○	○	○	○	—	○	—
S394	9	750	B	○	○	○	—	—	—	—
S306	5.5	800	A	○	○	○	—	—	—	—
S297	7.5	800	A	○	○	○	○	—	—	—
S402	8	800	B	○	○	○	○	—	○	—
S397	8.5	800	B	○	○	○	○	—	—	—
S395	9	800	A	○	○	○	—	—	—	○
S298	9.5	800	B	○	○	○	—	—	—	—
S351	10.5	800	B	○	○	○	—	—	—	○
S610	8	850	B	○	○	○	○	—	—	—
S709	8	900	S-400 + S-402	○	○	—	—	—	—	—
S358	10.5	900	B	○	○	—	—	—	—	—
S612	8	950	B	○	○	○	—	—	—	—

Notes: A = synthetic amphibolite, B = hydrous glass, and C = gel + H<sub>2</sub>O. ○ = present, — = absent, Grt = garnet, Omp = omphacite, Lws = lawsonite, Phen = phengite, Crn = corundum.



roxene at higher temperature (Fig. 2d). The larger garnet inclusions (>8 μm) in clinopyroxene porphyroblasts preserve the relict inner core formed at an earlier stage.

Lawsonite grows larger and is euhedral at high tem-

perature (Fig. 2e). No lawsonite was observed in run products from experiments carried out above 850 °C.

Glass was observed in lawsonite-absent charges; at 700 °C, 10 and 12.5 GPa, and at 800 °C, 9 and 10.5 GPa.

**FIGURE 2.** Backscattered electron images of experimental run products. G = garnet, Omp = omphacite (clinopyroxene), Si = SiO<sub>2</sub> phase, LW = lawsonite. The lengths of bars = 10 μm. (a) Clinopyroxene (omphacite) ranges in size from 5–20 μm. Two types of garnet are recognized; garnet having idiomorphic outlines ranging >3 μm in size, and newly formed garnet <2 μm. (b) Lawsonite is recognized in clinopyroxenes (omphacite) and in the matrix. (c) The porphyroblastic clinopyroxenes are fragmented, recognized as aggregates of the fiber shaped or sheaved crystals. Rounded reaction margins are also observed. (d) Idio-

morphic garnet crystals are commonly included in clinopyroxene at higher temperature. The larger garnet inclusions (>8 μm) in clinopyroxene porphyroblasts preserve the relict inner core formed at an earlier stage. (e) Lawsonite grows larger and occurs as euhedral crystals at higher temperature. (f) The glass is dominantly found with the SiO<sub>2</sub> phase aggregate >10–50 μm across. The SiO<sub>2</sub> phase does not have an idiomorphic outline. Matrix garnet is also included in the SiO<sub>2</sub> phase-dominant aggregates. The garnet is characterized by irregular anhedral rims, suggesting partial melting.

←

BSE images show that the glass is found mainly with the SiO<sub>2</sub> phase in aggregates more than 10–50 μm across (Fig. 2f). Matrix garnet is also included in the SiO<sub>2</sub> phase-dominant aggregates. The glass is distributed interstitially around the SiO<sub>2</sub> phase. The SiO<sub>2</sub> phase does not have an idiomorphic outline. It is noteworthy that the garnet is characterized by irregular anhedral rims, suggesting partial melting. If the glass was quenched from a melt, garnet and the SiO<sub>2</sub> phase should rather have the idiomorphic surfaces. An SiO<sub>2</sub> phase was observed in all runs except those at 8 GPa, 800 °C; 10.5 GPa, 900 °C; and at 8 GPa, 900 °C. The absence of an SiO<sub>2</sub> phase at higher temperatures may be due to the dissolution of SiO<sub>2</sub> into the fluid. The melt does not appear in the triple point defined by the silica phase, garnet, and clinopyroxene, which is one of the characteristic aspects of a partial melt that is different from fluids.

Moreover, the chemical composition of the glass is quite different from felsic melts. For example, the glass in the run product (S395) formed at 9.0 GPa, 800 °C is shown in Figure 2f. The glass is shown in the dark-colored portion that occupies the central part of the photo in a pentagonal region of about 50 μm across. It is composed of anhedral garnet (G), a mosaic of coesite, and glass, without clinopyroxene and lawsonite. The chemical composition of the glass is (in weight percent) SiO<sub>2</sub> = 78.64, Al<sub>2</sub>O<sub>3</sub> = 10.90, CaO = 4.64, FeO = 0.77, MgO = 0.36, and K<sub>2</sub>O = 0.01; Na<sub>2</sub>O is below the detection limit (Table 3). This is quite different from the felsic melt that is rich in albite component. The glasses of S358 formed at 10.5 GPa and 900 °C have a rhyolitic composition with SiO<sub>2</sub> = 75.88, although FeO = 2.42, MgO = 2.71, and CaO = 4.20 are too high compared to the liquids formed by the partial melting of eclogite.

Schmidt (1996) described the presence of fluid at pressures above the phengite breakdown (>10 GPa, < 1000 °C in the stishovite field) in the alkali basalt+H<sub>2</sub>O system. In the coesite field, phengite breakdown produces a melt. This is quite consistent with the present experimental result. That is, fluid is stable at pressures above the lawsonite breakdown in the stishovite field at temperatures ranging from 700 to 950 °C.

Other minor phases observed were corundum and phengite. Corundum was recognized at 800 °C, 8 GPa

and 750 °C, 8.5 GPa. Phengite was only observed at 700 °C, 5.5 GPa.

### MINERALOGY

Representative chemical compositions of run product phases (except phengite) are shown together with run conditions in Table 3. The chemical compositions of minerals without evidence of clear disequilibrium such as zoning or anhedral outlines were selected and plotted in a series of diagrams. Those are matrix-forming small grains or outermost rims of large euhedral crystals.

Lawsonites are close in composition to the ideal end-member, CaAl<sub>2</sub>Si<sub>2</sub>O<sub>8</sub>(2H<sub>2</sub>O). Minor amounts of Fe<sub>2</sub>O<sub>3</sub> (0.3–1.1 wt%), MgO (0.2–1.0 wt%), Na<sub>2</sub>O (0.3–0.6 wt%), and TiO<sub>2</sub> (0.2–0.4 wt%) are present in most cases.

Garnets are expressed by the grossular-pyrope-almandine components, and contain more than 55%, with the remaining components being majorite and NaTi garnet. Garnets formed in a wide range of *P* (5.5–13.5 GPa) and *T* (700–950 °C), and plot in a wide compositional range of almandine (27–60 mol%), grossular (19–47), and pyrope (17–42) components (Fig. 3).

At a constant temperature of 700 °C, the garnet X<sub>Mg</sub> tends to increase from 0.24 (8 GPa) to 0.41 (9.5 GPa) with a constant X<sub>Ca</sub> value, then the compositional trend is shifted sharply toward the grossular apex. This shift is consistent with the disappearance of lawsonite. The value of X<sub>Ca</sub> increases from 0.22 to 0.50 at constant X<sub>Mg</sub> as pressure increasing from 10.5 to 13.5 GPa (Fig. 3a).

At a constant pressure of 8 GPa, the compositional trend of garnet shows a kinked pattern similar to the isothermal (*T* = 700 °C) pressure-dependent trend. Values of X<sub>Mg</sub> increases from 0.25 (*T* = 700 °C) to 0.50 (*T* = 800 °C) at constant X<sub>Ca</sub>, then X<sub>Ca</sub> in garnet tends to increase toward the grossular apex at a constant X<sub>Mg</sub> value (Fig. 3b). The kink point coincides again with the *P-T* condition of the lawsonite-breakdown reaction.

Under the isothermal condition of 700 °C, the majorite (Mg<sub>4</sub>Si<sub>4</sub>O<sub>12</sub>) component in garnet increases with increasing pressure. The majorite component is expressed as the number of excess silicon cations above 3.0 pfu. It ranges from 3.13–3.34 Si pfu at 8 GPa to 3.46 Si pfu at 13.5 GPa.

At 16 GPa, the eclogite facies is separated by the gar-



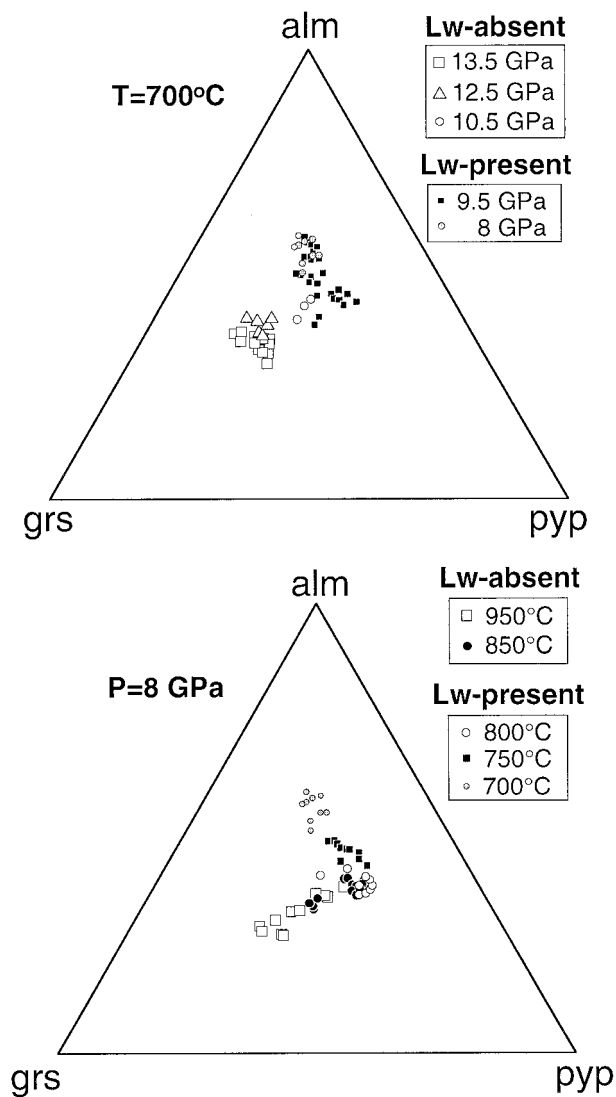


FIGURE 3. Garnet compositions portrayed in almandine-grossular-pyrope triangle. (a)  $T = 700\text{ }^{\circ}\text{C}$  (b)  $P = 8\text{ GPa}$ .

netite facies where omphacite disappears and majorite garnet becomes a stable monomineralic phase (Irifune et al. 1986). Under isothermal conditions at  $800\text{ }^{\circ}\text{C}$ , Si increases from 2.98–3.05 to 3.07–3.14 pfu with increasing pressure from 8 to 10.5 GPa. The transformation of orthopyroxene into majorite garnet was first documented experimentally by Akaogi and Akimoto (1977) in the  $\text{Mg}_4\text{Si}_4\text{O}_{12}$ - $\text{Mg}_3\text{Al}_2\text{Si}_3\text{O}_{12}$  and  $\text{Fe}_4\text{Si}_4\text{O}_{12}$ - $\text{Fe}_3\text{Al}_2\text{Si}_3\text{O}_{12}$  system. The present study indicates the continuous replacement of Ca-Mg-Fe components by majorite with increasing pressure below  $700\text{ }^{\circ}\text{C}$ , and supports the previous experimental result of pressure-dependent transformation of majorite garnet in the upper mantle transition zone.

Under isobaric conditions ( $P = 8\text{ GPa}$ ), Si decreases from 3.13–3.34 to 2.99–3.06 pfu of garnet with increasing temperature from 700 to  $950\text{ }^{\circ}\text{C}$ . The majorite com-

ponent goes down with increasing temperature. Thus, the majorite component is favored at higher  $P$ - $T$  conditions.

In contrast to the systematic compositional change of garnet, the clinopyroxene seems to be more scattered and less systematic with changing  $P$  and  $T$ . The pyroxene formula proportions were calculated based on six O atoms. The jadeite content is taken as being equal to the  $^{\text{VI}}\text{Al}$ . Clinopyroxenes all plot in the compositional field of omphacite ( $\text{Jd}_{35-47}\text{Aug}_{53-68}\text{Acm}_0$ ). The acmite component of clinopyroxene is negligibly small. At a constant pressure of 8 GPa, the mol% Jd in clinopyroxene tends to increase from 35 to 47 with increasing  $T$  from 700 to  $850\text{ }^{\circ}\text{C}$ . The mol% Jd tends to be stable at 35 with increasing  $P$  from 8 GPa to 12.5 GPa, and increases up to 39 at 13.5 GPa at a constant temperature of  $700\text{ }^{\circ}\text{C}$ . The full set of chemical composition of clinopyroxene is available upon request to the first author.

The Tschermak component of clinopyroxene, taken as  $^{\text{IV}}\text{Al}$ , ranges from 11 to 7 mol% with increasing  $P$  from 8 to 13.5 GPa. It decreases from 11.5 to 0 with increasing  $T$  from 700 through 850 to  $900\text{ }^{\circ}\text{C}$  at constant pressure of 8 GPa. Above  $900\text{ }^{\circ}\text{C}$ , it is negligibly small.

#### PHASE RELATIONS

The  $P$ - $T$  region of lawsonite stability determined in this study is shown by the two straight dashed lines in Figure 1. These two lawsonite-consuming reactions may join at a point slightly above 8 GPa, where the coesite-stishovite transition curve ties the two continuous reactions in the lawsonite-bearing MORB-water system. As discussed later in detail, the lawsonite-consuming reaction in the stishovite stability field is essentially the same as that in the coesite stability field except for the difference in the  $\text{SiO}_2$  polymorph. However, the stability field of the lawsonite eclogite assemblage delineated in Figure 1 must be examined by reversal experiments, due to the difficulty of demonstrating equilibrium owing to sluggish reaction, domain equilibrium, local variation of temperature distribution in a small capsule, and other unknown kinetic factors that may control the equilibrium.

To examine the degree of equilibrium, specifically for the lawsonite-out reaction boundary, two reversal experiments were conducted at conditions of 10 GPa and  $700\text{ }^{\circ}\text{C}$ , and at 8 GPa and  $900\text{ }^{\circ}\text{C}$  (Table 2). To reverse the lawsonite-out transformation, lawsonite-bearing assemblages synthesized first at 9.5 and 8 GPa,  $700\text{ }^{\circ}\text{C}$ , were held at  $700\text{ }^{\circ}\text{C}$  and 10 GPa. Two previous run products were mixed together to increase the volume of the starting mixture. The run product after 24 h showed the complete disappearance of the lawsonite, which locates the lawsonite stability field at  $700\text{ }^{\circ}\text{C}$ . A second reversal experiment was performed for the lawsonite-out reaction at lower pressures, using the mixtures of lawsonite-bearing assemblages synthesized first at 750 and  $800\text{ }^{\circ}\text{C}$ , at 8 GPa. Lawsonite disappeared at  $900\text{ }^{\circ}\text{C}$  and 8 GPa, which is beyond the lawsonite stability field. These reversal experiments confirm the location of the lawsonite-out reaction shown in Figure 1.

Strong chemical zonation in garnet is only observed in run products formed at  $T$  higher than 850 °C. With the exception of those garnets in run charges formed at  $T$  higher than 850 °C, most rock-forming minerals are not systematically zoned. However, chemical compositions are variable almost grain by grain to some extent. If no clear textural evidence for disequilibrium was observed, we assumed that the mineral compositions were in equilibrium with matrix phases. Chemically variable mineral compositions may be due to local domain equilibrium, temperature gradients within a capsule, disequilibrium by sluggish reaction kinetics, or some combinations of these factors. Despite these difficulties, the results indicate that equilibrium was obtained, to a first-order approximation, as judged by the phase relations and the Fe/Mg partitioning between garnet and clinopyroxene in run products. The garnet-clinopyroxene pairs that were either in contact or within two micrometers of each other were selected as equilibrium pairs. The results show that the isobaric ( $P = 8$  GPa)  $\ln K_D$  values decrease from 2.5 (700 °C), through 1.3 (750 °C) to 1.0 (800 °C). The trend of decreasing  $\ln K_D$  with increasing  $T$  is consistent with the results of Ellis and Green (1979) and other studies, although the  $K_D$  values are quantitatively different from, say, the equation by Ellis and Green (1979). The present isobaric  $\ln K_D$  values, e.g., at 700 °C, were plotted on their reference lines ranging from 900 to 1200 °C. A fairly large discrepancy is obtained mainly from pressure differences. Their experiments were done at pressures lower than 3 GPa, whereas ours were mainly 7.5–12.5 GPa. Their pressure calibration is limited to less than 3 GPa.

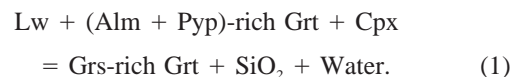
Analytical spread of the  $\ln K_D$  values in the present experiment is quite compatible with the experiment of Ellis and Green (1979; see their Fig. 3). This is partly due to experimental error of  $P$ - $T$  estimates, failure to attain equilibrium, compositional heterogeneity, minor thermal gradients in the capsules, uncertainties of chemical analysis, and estimate of  $\text{Fe}^{3+}$  of the run products, in addition to the unknown pressure effect of the proposed equations of Ellis and Green (1979).

The isothermal phase relations at 700 °C are shown on a ternary conventional ACFM diagram in Figure 4. The starting bulk composition has 10 components ( $\text{SiO}_2$ - $\text{TiO}_2$ - $\text{Al}_2\text{O}_3$ - $\text{Fe}_2\text{O}_3$ - $\text{FeO}$ - $\text{MgO}$ - $\text{CaO}$ - $\text{Na}_2\text{O}$ - $\text{K}_2\text{O}$ - $\text{H}_2\text{O}$ ) (Table 1); however,  $\text{TiO}_2$  is a minor trace component, which is mainly present in rutile.  $\text{Na}_2\text{O}$  is present only in the jadeite component of omphacite.  $\text{K}_2\text{O}$  is minor and mainly present in phengite. Garnet and clinopyroxene in the run product contain traces of  $\text{Fe}_2\text{O}_3$ . The  $\text{FeO}/\text{MgO}$  ratio of the starting bulk composition was fixed; thus compositions can be reduced to three components [ $(\text{Al}_2\text{O}_3 + \text{Fe}_2\text{O}_3 - \text{Na}_2\text{O})$ - $\text{CaO}$ - $(\text{FeO} + \text{MgO})$ ], with an excess  $\text{SiO}_2$  phase (either coesite or stishovite) and an  $\text{H}_2\text{O}$ -rich fluid (Fig. 4). At 8 GPa, the three-phase assemblage  $\text{Grt} + \text{Cpx} + \text{Lw}$  is stable. With increasing pressure, the compositional enlargement of garnet toward grossular end-member is obvious in this diagram.

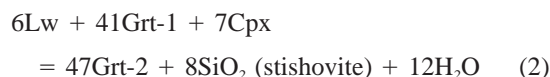
The tie lines between Grt and Cpx with excess Lw

rotate toward Lw with increasing pressure. When they reach the bulk-chemical composition shown as a large solid circle at 10 to 10.5 GPa, lawsonite disappears. A slight discrepancy exists in the  $P$ - $T$  condition of lawsonite disappearance, i.e., in spite of the absence of lawsonite in the run product at 10 GPa, the bulk composition falls in the Lw-Grt-Cpx triangle, although it is very close to the tie line. The tie lines between Grt and Cpx in all run products above 10.5 GPa are always on the bulk-chemical composition (Fig. 4). The minor discrepancy may be derived from the compositional variation of garnet, specifically an (Alm+Pyp)-rich composition due to local equilibrium, or that possible minor lawsonite avoided detection.

The systematic compositional enlargement of the garnet solid solution toward the grossular end-member is present with increasing pressure. The values of  $X_{\text{Ca}}$  increases under the buffered assemblage from 0.22 (8 GPa), through 0.26 (9.5 GPa), 0.30 (10.5 GPa), and 0.42 (12.5 GPa), to 0.44 (13.5 GPa). Lawsonite disappears between 9.5 and 10.5 GPa. This type of reaction leading to the disappearance of lawsonite is continuous, and is expressed by the following reaction;



By comparing the chemical compositions between 8.0 GPa and 10.5 GPa, the above reaction can be calculated as:



where Grt-1 and Grt-2 refer to the compositions at 8 and 10.5 GPa, respectively (Fig. 5).

With further increases in pressure, garnet tends toward the majorite component. In other words, the garnet composition moves toward the bulk-chemical composition with increasing pressure such that by 16 GPa, a monomineralic majoritic-garnet composition would be expected (Irifune et al. 1986). The isobaric phase relations show the same tendency as the isothermal relations.

#### A NEW PHASE DIAGRAM OF MORB+H<sub>2</sub>O SYSTEM

The present study defines the high-pressure stability limit of lawsonite in the MORB+H<sub>2</sub>O system (Figs. 1 and 6). The lawsonite-eclogite facies is bounded by the high-pressure stability limit of a lawsonite-bearing continuous reaction defined by the compositional enlargement of garnet toward the grossular-rich end-member with increasing pressure and/or temperature. Lawsonite is stable in metabasites up to 10 GPa and lower than 900 °C.

The eclogite facies is subdivided into four subfacies (Fig. 6). The dry eclogite facies has the largest  $P$ - $T$  space and is bounded by the garnetite facies at  $P > 16$  GPa (Irifune et al. 1986) and by the dry solidus at high  $T$ . The low-pressure limit of lawsonite-bearing eclogite facies is bounded by the epidote eclogite subfacies by a boundary

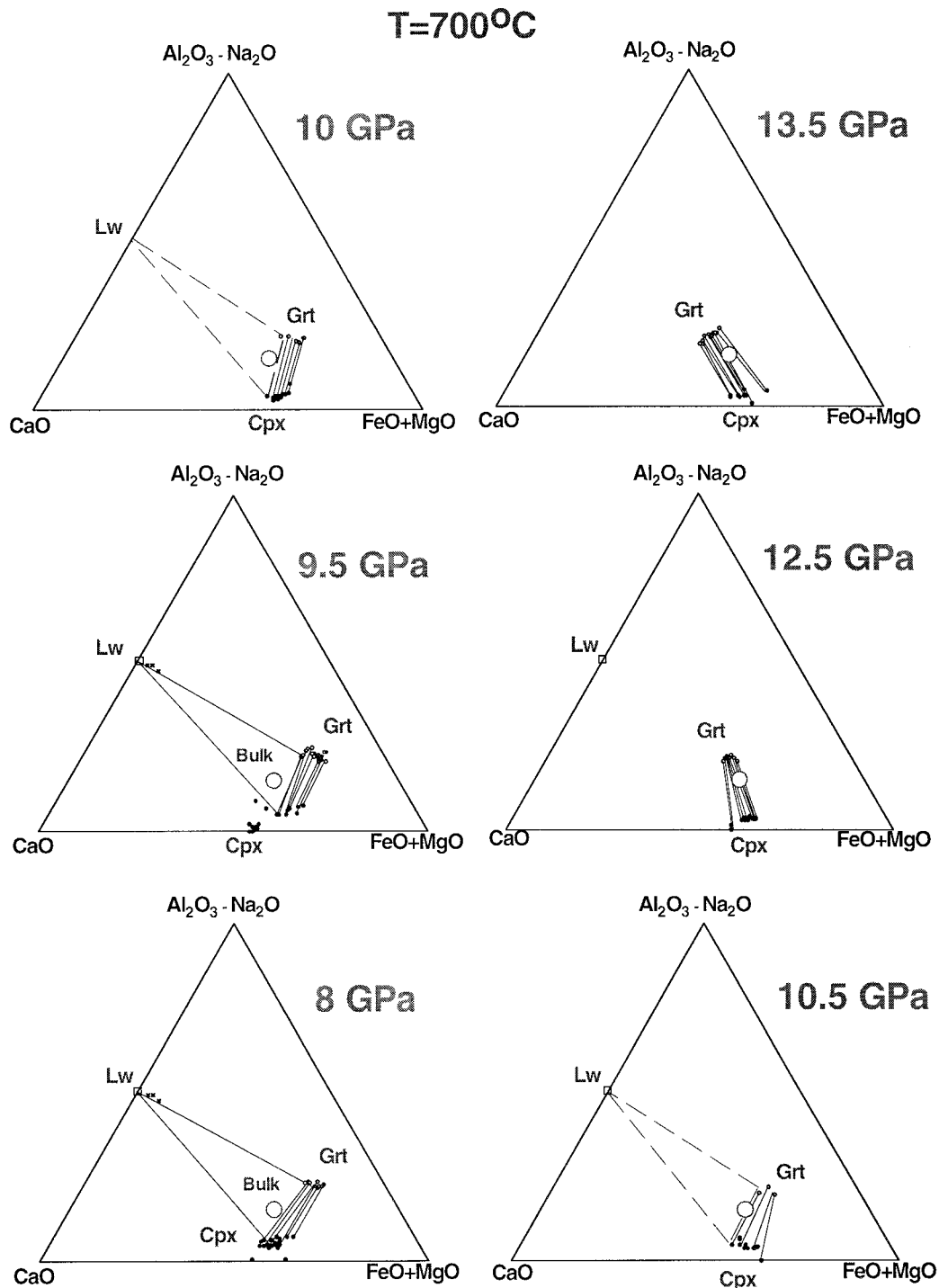


**FIGURE 4.** AC(FM) diagram showing the isothermal transition from lawsonite eclogite facies to dry eclogite facies with increasing pressures ( $T = 700^\circ\text{C}$ ). A =  $\text{Al}_2\text{O}_3\text{-Na}_2\text{O}$ , C = CaO, and FM = FeO+MgO. Note the phase relations in relation to bulk composition shown by the larger circle.

reaction with a gentle positive slope at 2–3 GPa (Poli and Schmidt 1995). The low-pressure and low-temperature boundary is separated from the blueschist facies by a reaction curve with a gentle negative Clapeyron slope (Ma-

ruyama 1997). The amphibole eclogite subfacies is stable below the epidote (zoisite) eclogite subfacies, down to 1.0 GPa. Both the epidote (zoisite)- and amphibole-eclogite subfacies are terminated by the slab-melting curves

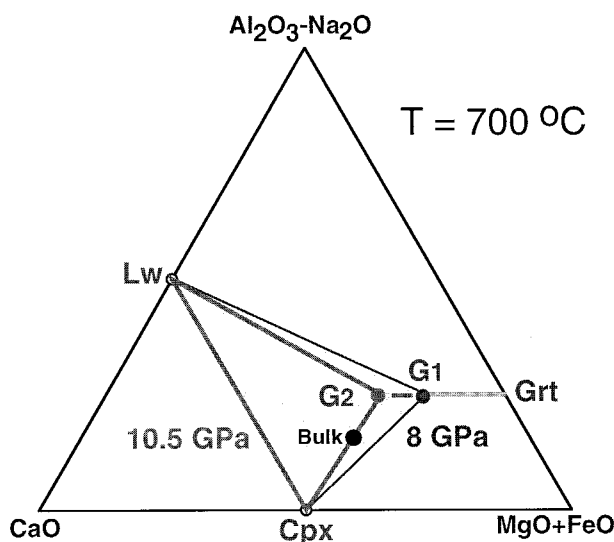
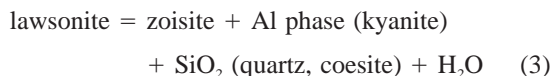


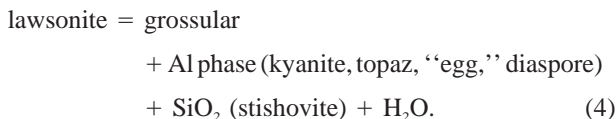
FIGURE 5. Schematic representation of the lawsonite-consuming reaction in the AC(FM) system.

at the high  $T$  side (Fig. 6). The metamorphic facies below 2.0 GPa are after Maruyama (1997).

The stability field of lawsonite in the CASH system (Schmidt 1995) is significantly larger than in the MORB+H<sub>2</sub>O system (Figs. 1 and 6). These differences have already been described in Pawley (1993), Schmidt (1995), and Poli and Schmidt (1995, 1997), and may be explained by the addition of FeO+MgO causing: (1) dilution of grossular by pyrope and almandine in a garnet solid solution, thereby reducing the activity of grossular, and (2) crystallization of clinopyroxene, displacing the lawsonite-consuming reactions to lower pressures and temperatures. In the CASH system, lawsonite break-down reactions are described as:



or



In the following, the fate of water from mid-oceanic ridge to subduction zone is discussed, based on the newly proposed phase diagram and additional laboratory-field constraints.

#### WATER IN THE OCEANIC CRUST

New oceanic crust is created at the mid-oceanic ridge and suffers hydrothermal fluid-alteration (Miyashiro 1973). The oceanic crust generated at the mid-oceanic ridge is about 7 km thick, and the top 600–700 m are hydrated by reaction with circulating hydrothermal water. Beneath 700 m, the crust is essentially dry except along

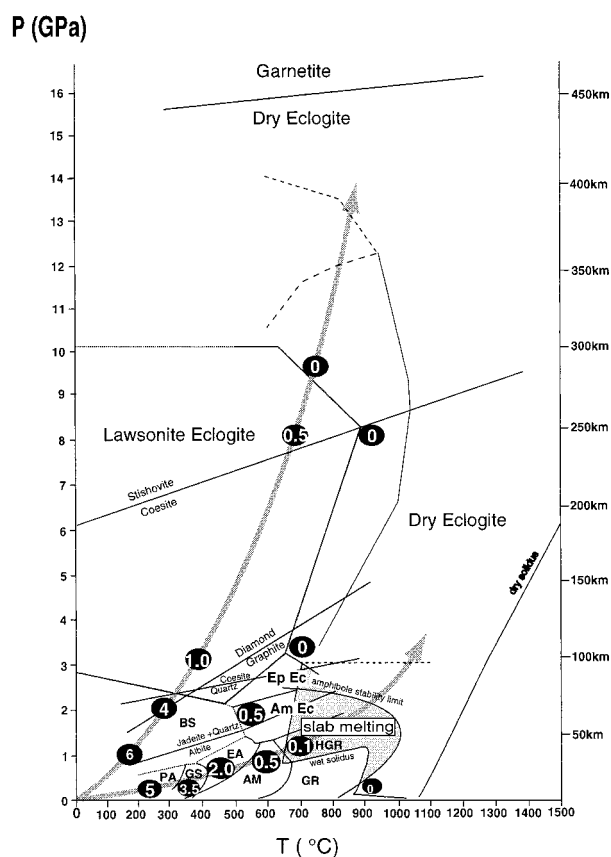


FIGURE 6.  $P$ - $T$  diagram showing the temperature distribution on the Benioff surface and the estimated H<sub>2</sub>O wt% of the subducting oceanic crust (circled number). The H<sub>2</sub>O wt% below the eclogite facies is from Peacock (1993). The calculated H<sub>2</sub>O wt% in the lawsonite eclogite facies is from Poli and Schmidt (1995) and this study. Abbreviations: PA = pumpellyite-actinolite facies, GS = greenschist facies, EA = epidote-amphibolite facies, AM = amphibolite facies, GR = granulite facies, HGR = high-pressure granulite facies, BS = blueschist facies, Am Ec = amphibole eclogite facies, and Ep Ec = epidote eclogite facies. Diamond-graphite curve is after Bundy (1980). Jadeite-quartz-albite equilibria is after Newton and Smith (1967) for low albite and Holland (1980) for high albite. The other index reaction curves are same as Figure 1. For more details, see Maruyama et al. (1996) and Maruyama (1997).

fracture zones. The H<sub>2</sub>O added to the oceanic crust by hydrothermal metamorphism is difficult to estimate precisely. Water is present both as loosely bound (H<sub>2</sub>O<sup>-</sup>) and structurally bound molecular water (H<sub>2</sub>O<sup>+</sup>). The measured structural water from the DSDP hole 504B (Alt et al. 1986) is approximately 1–2 wt% from the top of the pillow lava zone down to 600 m. However, it increases to 4–6 wt% from 600 down to 800 m depth (the transitional zone from the pillow to the dike zone). The structural water of dredged basaltic samples has been estimated to range from 1 to 8 wt% (Hart 1976). Staudigel et al. (1995) estimated the structural water content at the crust at about 2.7 wt% and the interstitial water as at least

2 wt%, on the basis of the void volume of the crust [estimated at approximately 5 vol% by Johnson (1979)]. The present study uses 6 wt%  $\text{H}_2\text{O}^+$ , which is stored in hydrous minerals due to ocean-floor hydrothermal metamorphism.

Dredged gabbros and ultramafic rocks from fracture zones are highly altered and suffer high-grade greenschist to amphibolite facies metamorphism. These rocks contain several hydrous minerals. However, such hydrated rocks are restricted to fracture zones. Oceanic crust is subsequently subducted at convergent plate margins. Fluid trapped in the pore space of the subducting oceanic crust and overlying sediments is expelled within the top 10–15 km (e.g., Moore 1992). Loosely bound water ( $\text{H}_2\text{O}^-$ ) is also released at shallow depths, probably between 15 to 20 km. Afterward, the subducted oceanic crust suffers subduction-zone metamorphism and continues to release  $\text{H}_2\text{O}$  by dehydration reactions to the overlying mantle wedge.

To estimate the water content of subducting oceanic crust, we have combined our results with the previous estimates of Poli and Schmidt (1995) and Peacock (1993) to produce Figure 6. Previous experimental studies have demonstrated that the subducting oceanic crust releases most of its  $\text{H}_2\text{O}$  by the amphibolite-eclogite transformation at 75 km depth and retains <1 wt%  $\text{H}_2\text{O}$  beneath the volcanic front about 100 km depth if the temperature is below 650 °C. However, if the temperature is above 650 °C, at 30–80 km, subducting oceanic crust reaches the solidus temperature condition, causing the partial melting of amphibole-bearing metamorphosed oceanic crust. The released  $\text{H}_2\text{O}$  moves into the melt; the remaining subducting oceanic crust transforms to dry eclogite. Once it turns to dry eclogite, the crust never melts due to the abnormally high- $T$  solidus of more than 1500 °C at 200 km depth.

The  $\text{H}_2\text{O}$  content in the subducting oceanic crust depends on the variation of the  $P$ - $T$  path of the Benioff surface. In the case of subduction of a very old oceanic plate along an extremely low geothermal gradient (2–3 °C/km), the subducting oceanic crust suffers progressive high  $P$ - $T$  metamorphism from blueschist to lawsonite eclogite facies. Lawsonite-eclogite facies assemblages are stable in a  $P$ - $T$  field extending from 2.5 GPa, <500 °C, through 8 GPa, <800 °C to 9.5 GPa, <700 °C. That is, lawsonite is stable at depths ranging from 75 km to 300 km. Lawsonite is continuously dehydrated with increasing temperature in the coesite field, and with increasing pressure and temperature in the stishovite field. Extremely old oceanic plate subduction releases 3 wt%  $\text{H}_2\text{O}$  continuously from 75 km to 100 km depth by the blueschist-lawsonite eclogite transformation and retains 1 wt%  $\text{H}_2\text{O}$  in the subducting slab (Fig. 6). At the depths of the lawsonite eclogite facies, continuous dehydration of lawsonite releases small quantities of the remaining  $\text{H}_2\text{O}$ ; the subducting oceanic crust retracts ~0.5 wt%  $\text{H}_2\text{O}$  even at depths >200 km. In the stishovite field, the descending

slab continuously releases all  $\text{H}_2\text{O}$  at the lawsonite eclogite stability limit, at 300 km depth.

#### ACKNOWLEDGMENTS

The authors express sincere thanks to E. Takahashi for the use of his multi-anvil facilities. Eiichi Takahashi, J.G. Liou, and M. Schmidt gave us useful comments and suggestions. Ichiro Aoki gave me valuable suggestions on the XRD analyses and the modal calculation of run products. We thank the above named individuals for their help and discussion.

#### REFERENCES CITED

- Akaogi, M. and Akimoto, S. (1977) Pyroxene-garnet solid-solution equilibria in the system  $\text{Mg}_2\text{Si}_4\text{O}_{12}$ - $\text{Mg}_3\text{Al}_2\text{Si}_3\text{O}_{12}$  and  $\text{Fe}_3\text{Si}_4\text{O}_{12}$ - $\text{Fe}_3\text{Al}_2\text{Si}_3\text{O}_{12}$  at high pressures and temperatures. *Physics of the Earth and Planetary Interior*, 15, 90–106.
- Alt, J.C., Honnorez, J., Laverne, C., and Emmermann, R. (1986) Hydrothermal alteration of a 1 km section through the upper oceanic crust, deep sea drilling project Hole 504B: Mineralogy, chemistry, and evolution of seawater-basalt interactions. *Journal of Geophysical Research*, 91, 10,309–10,335.
- Bohlen, S.R. and Boettcher, A.L. (1982) The quartz-coesite transformation: A precise determination and the effects of other components. *Journal of Geophysical Research*, 87, 7073–7078.
- Brophy, J.G. and Marsh, B.D. (1986) On the origin of high-alumina arc basalt and the mechanics of melt extraction. *Journal of Petrology*, 27, 763–789.
- Bundy, F.R. (1980) The  $P$ ,  $T$  phase reaction diagrams for elemental carbon. *Journal of Geophysical Research*, 85, 6930–6936.
- Caron, J.M. and Pequignot, G. (1986) The transition between blueschists and lawsonite-bearing eclogites based upon observations from Corsican metabasites. *Lithos*, 19, 205–218.
- Chopin, C. and Sobolev, N.V. (1995) Principal mineralogical indicators of UHP in crustal rocks. In R.G. Coleman and X. Wang, Eds., *Ultrahigh Pressure Metamorphism*, p. 96–131. Cambridge University Press, Cambridge, U.K.
- Delany, J.M. and Helgeson, H.C. (1978) Calculation of the thermodynamic consequences of dehydration in subducting oceanic crust to 100 kb and >800°C. *American Journal of Sciences*, 278, 638–686.
- Ellis, D.J. and Green, D.H. (1979) An experimental study of the effect of Ca upon garnet-clinopyroxene Fe-Mg exchange equilibria. *Contributions to Mineralogy and Petrology*, 71, 13–22.
- Ghent, E.D., Stout, M.Z., and Erdmer, P. (1993) Pressure-temperature evolution of lawsonite-bearing eclogites, Pinchi Lake, British Columbia. *Journal of Metamorphic Geology*, 11, 279–290.
- Hart, R.A. (1976) Progressive alteration of the oceanic crust. In R.S. Yeats and S.R. Hart et al., Eds., *Initial Reports of the Deep Sea Drilling Project*, 34, 433–437.
- Helmstaedt, H. and Doig, R. (1975) Eclogite nodules from kimberlite pipes of the Colorado Plateau—samples of subducted Franciscan-type oceanic lithosphere. *Physics and Chemistry of the Earth*, 9, 95–111.
- Helmstaedt, H. and Schulze, D.J. (1988) Eclogite-facies ultramafic xenoliths from Colorado Plateau diatreme breccias: Comparison with eclogites in crustal environments, evaluation of the subduction hypothesis, and implications for eclogite xenoliths from diamondiferous kimberlites. In D.C. Smith, Ed., *Eclogites and eclogite facies rocks*, p. 387–450. Elsevier Science, Amsterdam.
- Holland, T.J.B. (1980) The reaction albite = jadeite + quartz determined experimentally in the range 600–1200 °C. *American Mineralogist*, 65, 125–134.
- Inoue, T., Yurimoto, H., and Kudoh, Y. (1995) Hydrous modified spinel,  $\text{Mg}_{1.75}\text{SiH}_{0.5}\text{O}_4$ : a new water reservoir in the mantle transition region. *Geophysical Research Letters*, 22, 117–120.
- Irfune, T., Sekine, T., and Ringwood, A.E. (1986) The eclogite-garnetite transformation at high pressure and some geophysical implications. *Earth and Planetary Science Letters*, 77, 245–256.
- Ito, E., Takahashi, E., and Matsui, Y. (1984) The mineralogy and chemistry of the lower mantle: an implication of the ultrahigh-pressure phase relations in the system  $\text{MgO}$ - $\text{FeO}$ - $\text{SiO}_2$ . *Earth and Planetary Science Letters*, 67, 238–248.

- Johnson, D.M. (1979) Crack distribution in the upper oceanic crust and its effects upon seismic velocity, seismic structure, formation permeability, and fluid circulation. In T. Donnelly et al., Eds., *Initial Reports of the Deep Sea Drilling Project*, 1473–1490.
- Kawamoto, T., Hervig, R.L., and Holloway, J.R. (1996) Experimental evidence for a hydrous transition zone in the early Earth's mantle. *Earth and Planetary Science Letters*, 142, 587–592.
- Liou, J.G., Zhang, R., and Ernst, W.G. (1994) An introduction to ultrahigh-pressure metamorphism. *The Island Arc*, 3, 1–24.
- Maruyama, S. (1997) Pacific-type orogeny revisited: Miyashiro-type orogeny proposed. *The Island Arc*, 6, 91–120.
- Maruyama, S., Liou, J.G., and Terabayashi, M. (1996) Blueschists and eclogites of the world and their exhumation. *International Geology Review*, 38, 485–594.
- Miyashiro, A. (1973) *Metamorphism and metamorphic belts*, 492 p. Wiley, New York.
- Moore, C.J. (1992) Fluids in accretionary prisms. *Reviews of Geophysics*, 30, 113–135.
- Newton, R.C. and Smith, J.V. (1967) Investigations concerning breakdown of albite at depth in the earth. *Journal of Geology*, 45, 268–286.
- Nicolls, I.A. and Ringwood, A.E. (1973) Effect of water on olivine stability in tholeiites and production of silica-saturated magmas in the island arc environment. *Journal of Geology*, 81, 285–300.
- Okamoto, K. and Maruyama, S. (1998) Multi-anvil re-equilibration experiments of a Dabie Shan UHP eclogite within the diamond-stability fields. *The Island Arc*, 7, 52–69.
- Parkinson, C.D., Miyazaki, K., Wakita, K., Barber, A.J., and Carswell, D.A. (1998) An overview and tectonic synthesis of the pre-Tertiary very-high-pressure metamorphic and associated rocks of Java, Sulawesi and Kalimantan, Indonesia. *The Island Arc*, 7, 184–200.
- Pawley, A.R. (1994) The pressure and temperature stability limits of lawsonite: Implications for H<sub>2</sub>O recycling in subduction zones. *Contributions to Mineralogy and Petrology*, 118, 99–108.
- Peacock, S.M. (1993) The importance of blueschist—eclogite dehydration reactions in subducting oceanic crust. *Geological Society of America Bulletin*, 105, 684–694.
- Poli, S. (1993) The amphibolite-eclogite transformation: An experimental study on basalt. *American Journal of Science*, 293, 1061–1107.
- Poli, S. and Schmidt, M.W. (1995) H<sub>2</sub>O transport and release in subduction zones: Experimental constraints on basaltic and andesitic systems. *Journal of Geophysical Research*, 100, 22,299–22,314.
- (1997) The high-pressure stability of hydrous phases in orogenic belts: an experimental approach on eclogite-forming processes. *Tectonophysics*, 273, 169–184.
- Ringwood, A.E. (1975) *Composition and petrology of the Earth's mantle*. McGraw-Hill, New York.
- Schmidt, M.W. (1995) Lawsonite: Upper pressure stability and formation of higher density hydrous phases. *American Mineralogist*, 80, 1286–1292.
- (1996) Experimental constraints on recycling of potassium from subducted oceanic crust. *Science*, 272, 1927–1930.
- Schmidt, M.W. and Poli, S. (1994) The stability of lawsonite and zoisite at high pressure: Experiments in CASH to 92 kbar and implications for the presence of hydrous phases in subducted lithosphere. *Earth and Planetary Science Letters*, 124, 105–118.
- Schreyer, W. (1988) Experimental studies on metamorphism of crustal rocks under mantle pressures. *Mineralogical Magazine*, 52, 11–26.
- (1995) Ultradeep metamorphic rocks: The retrospective viewpoint. *Journal of Geophysical Research*, 100, No. B5, 8353–8366.
- Shido, F. and Miyashiro, A. (1971) Crystallization of abyssal tholeiites. *Contributions to Mineralogy and Petrology*, 31, 251–266.
- Smyth, J.R. and Kawamoto, T. (1997) Wadsleyite II: A new high pressure hydrous phase in the peridotite-H<sub>2</sub>O system. *Earth and Planetary Science Letters*, 146, E9–E16.
- Staudigel, H., Davies, G.R., Hart, S.R., Marchant, K.M., and Smith, B.M. (1995) Large scale isotopic Sr, Nd and O isotopic anatomy of altered oceanic crust: DSDP/ODP sites 417/418. *Earth and Planetary Science Letters*, 130, 169–185.
- Takahashi, E., Shimazaki, T., Tsuzaki, Y., and Yoshida, H. (1993) Melting study of a peridotite KLB-1 to 6.5 GPa, and the origin of basaltic magmas. *Philosophical Transactions of the Royal Society of London A*, 342, 105–120.
- Tatsumi, Y., Hamilton, D.L., and Nesbitt, R.W. (1986) Chemical characteristics of fluid phase released from a subducted lithosphere and origin of arc magmas: Evidence from high-pressure experiments and natural rocks. *Journal of Volcanology and Geothermal Research*, 29, 293–309.
- Wyllie, P.J. (1988) Magma genesis, plate tectonics, and chemical differentiation of the Earth. *Review of Geophysics*, 26, 370–404.
- Wyllie, P.J. and Sekine, T. (1982) The formation of mantle phlogopite in subduction hybridization. *Contributions to Mineralogy and Petrology*, 79, 375–380.
- Zhang, J., Li, B., Utsumi, W., and Liebermann, R.C. (1996) In situ X-ray observations of the coesite-stishovite transition: reversed phase boundary and kinetics. *Physics and Chemistry of Minerals*, 23, 1–10.

PAPER RECEIVED MAY 14, 1998

PAPER ACCEPTED SEPTEMBER 26, 1998

PAPER HANDLED BY DAVID M. JENKINS